Introducing Dimensionality to the Archetypical Mn_{12} Single-Molecule Magnet: a Family of $[Mn_{12}]_n$ Chains

Sergio A. Corrales,[†] John M. Cain,[†] Kelley A. Uhlig,[†] Andrew M. Mowson,[‡]
Constantina Papatriantafyllopoulou,[§] Marcus K. Peprah,[⊥] Andrew Ozarowski,[∥]
Anastasios J. Tasiopoulos,[§] George Christou,[‡] Mark W. Meisel,[⊥] and Christos Lampropoulos*,[†]

[†]Department of Chemistry, University of North Florida, 1 UNF Drive, Jacksonville, Florida 32224, United States

[‡]Department of Chemistry, University of Florida, Gainesville, Florida 32611-7200, United States

[§]Department of Chemistry, University of Cyprus, 1678 Nicosia, Cyprus

[⊥]Department of Physics and National High Magnetic Field Laboratory (NHMFL), University of Florida, Gainesville, Florida 32611-8440, United States

[∥]National High Magnetic Field Laboratory (NHMFL), Florida State University, Tallahassee, Florida 32310, United States

S *Supporting Information*

ABSTRACT: The $[Mn_{12}O_{12}(O_2CR)_{16}(L_4)]$ family (R = various; L = terminal ligand) of clusters holds a special place in molecular magnetism; they are the most well-studied single-molecule magnets (SMMs). Targeted linkage of these SMMs has now been achieved for the first time. The resulting chain structures have been confirmed crystallographically, and the magnetic properties, up to 1.14 GPa, and high-field electron paramagnetic resonance spectra have been collected and analyzed.

Single-molecule magnets (SMMs) are nanoscopic super-paramagnetic particles that owe their properties to the combination of a well-isolated high-spin ground state and significant axial anisotropy.[1] A number of transition-metal clusters have been recognized as SMMs, and Mn-based species have been central in the development of this field because of their Jahn−Teller (JT)-distorted Mn^{III} ions.[2] The first family of SMMs, i.e., the lineage of clusters described by the general formula $[Mn_{12}O_{12}(O_2CR)_{16}(L_4)]$ (R = various; L = terminal ligand), still remains the most well-studied.[3] A range of experimental physics studies have shown SMMs to be true mesoscale species, exhibiting the classical properties of magnets, i.e., magnetization versus field hysteresis loops, as well as quantum properties, i.e., quantum tunneling of magnetization, quantum phase interference, and other phenomena, where the Mn_{12} family has been the model system.[4]

As such, it has been a long-sought-after goal of chemists involved in molecular magnetism to synthesize oligomers or polymers of Mn_{12} SMMs, especially after exchange bias effects were identified in a handful of smaller SMM oligomeric species[5] and linkage of small SMMs into extended structures was accomplished.[6] However, targeted linking of Mn_{12} SMMs has not been achieved to date. Herein we report the deliberate introduction of dimensionality into Mn_{12} SMMs, with the installation of bifunctional diol ligands at sites occupied by neutral terminal ligands, namely, water or other solvents.[7] Retaining the Mn_{12} core was essential, so mild room-temperature reaction conditions were employed. The first diol utilized was

2-butyne-1,4-diol, and the resulting structure is presented in Figure 1A.

The synthetic route involves the reaction of 2-butyne-1,4-diol, $[Mn_{12}O_{12}(O_2CMe)_{16}(H_2O)_4]\cdot MeCOOH\cdot 4H_2O$ ($Mn_{12}Ac$),[8] and Bu^tCH_2COOH in MeCN. From this reaction mixture, X-ray-quality single crystals of $[Mn_{12}O_{12}(O_2CCH_2Bu^t)_{16}(L_1)_3]_n$ (**1**; L_1 = 2-butyne-1,4-diol) emerged. The structure (Figure 1A) shows that, as targeted, the diol has linked the Mn_{12} clusters, leading to the formation of one-dimensional (1D) chains of Mn_{12} building blocks. This is the first 1D covalently linked chain of Mn_{12} units. There are four diols on each Mn_{12}, of which two act as linkers and two are terminal. The $[Mn_{12}O_{12}]^{16+}$ core, which includes a $[Mn^{IV}_4]$ cubane unit surrounded by a ring of eight Mn^{III} ions, is nearly unaltered. The structure resembles a zigzag chain. The terminal diols are hydrogen-bonded to terminal diols of neighboring chains and form a two-dimensional (2D) network of covalently linked chains connected via interchain hydrogen bonds (Figure S1).
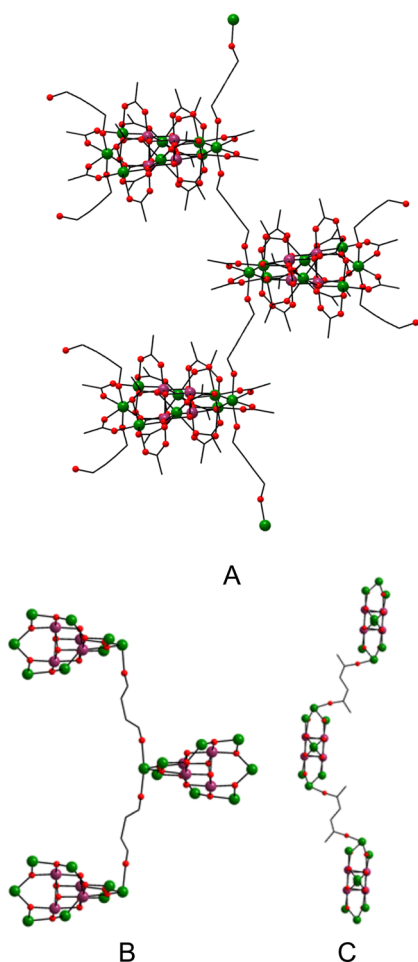
The effect of the ligand bulk on chain formation was then investigated, including the length, structural rigidity, and conjugation of the ligand backbone. The use of *cis*-2-butene-1,4-diol produced a 1D covalently bound chain of Mn_{12} building blocks, namely, $[Mn_{12}O_{12}(O_2CCH_2Bu^t)_6(L_3)]$ (**2**; L_2 = *cis*-2-butene-1,4-diol). Similar to **1**, complex **2** also features two hydrogen bonds per Mn_{12}, which overall leads again to a supramolecular 2D network. It is noted here that, in both **1** and **2**, the Mn_{12} core's anisotropy axis (easy axis) is oriented parallel to the chain direction (Figures 1 and S2). Evidently, the subtle differences between the two diols in **1** and **2** are not sufficient to cause significant structural changes because similar chains resulted.

Therefore, some structural strain was introduced by using 2,5-hexanediol, in which case two branching methyl groups are symmetrically adjacent to the two alcohol moieties, while the backbone is saturated. As is evident from Figure 1C, the crystal structure of the resulting $[Mn_{12}O_{12}(O_2CCH_2Bu^t)_{16}(L_3)$-

Figure 2. Out-of-phase ac susceptibility plots for **1−3**.

The intra- and interchain interactions between Mn_{12} building blocks are expected to be weak because of the nature of the linkage. Thus, we undertook a practical approach to investigate this interaction, if any, by attempting to observe changes in the intermolecular Mn_{12} communication by applying pressure. For this study, representative complex **1** was investigated in a home-built pressure cell, and a piece of Pb was used as a manometer.[9] The isothermal hysteresis measurement involved sweeping the magnetic field between ± 7 T at 2 K. At ambient pressure, a coercive field (H_c) of 1.35 T was observed (Figure 3). A step is
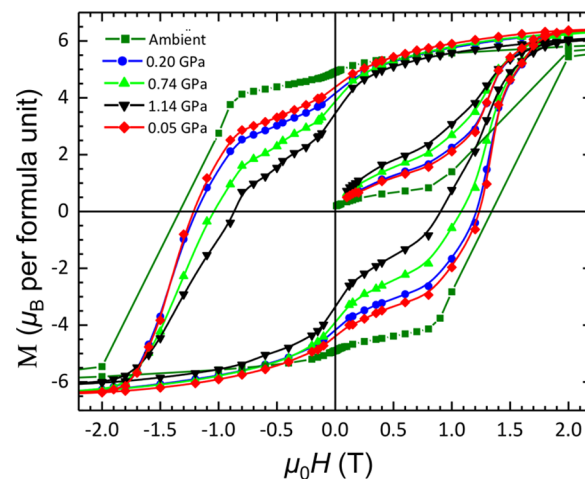
Figure 3. Isothermal magnetic hysteresis loops ($T = 2$ K) for **1**, in chronological order, at ambient and elevated pressures. The low-field (< ± 100 mT) data are omitted when Pb is present (see the text). Solid lines are guides for the eyes.

$(H_2O)_2]_n$ (**3**; L_3 = 2,5-hexanediol), the ligand's bulk had a profound effect on the chain, with the Mn_{12} SMM's easy axis now perpendicular to the chain direction. Another difference between **3** and **1/2** is the absence of terminal diols; instead, complex **3** has two five-coordinate Mn^{III} ions. This results in the absence of hydrogen bonds with neighboring chains, so **3** is the first true 1D chain, free of noncovalent interchain linkages. Ergo, the identity of the linker affects the overall structure. The distance between building blocks is reported as the distance between the Mn^{3+} ions bridged by the linker. The smallest distance is that of **3** (8.1 Å), in which the Mn_{12} building blocks are "flipped". The intermolecular intrachain distances in **1** and **2** are 10.0 and 9.7 Å, respectively.

Variable-temperature direct-current (dc) and alternating-current (ac) magnetic susceptibility studies were performed on complexes **1−3**, and in all cases, they suggest an $S = 10$ ground-state spin, which is the expected spin of the Mn_{12} building block. The out-of-phase ac magnetic susceptibility plots (Figure 2) reveal common features, namely, one set of frequency-dependent ac peaks at high temperatures (at ∼8 K for **1**, at ∼7.9 K for **2**, and at ∼5 K for **3** at 1500 Hz) and one set of frequency-dependent ac peaks at lower temperatures (at ∼3.2 K for **1** and **2** and at ∼2 K for **3** at 1500 Hz). Both sets of ac peaks are frequency-dependent, which is not surprising because the Mn_{12} building unit is a SMM and intermolecular interactions are expected to be weak.

also observed near $H = 0$, which corresponds to a critical field at which resonant magnetization tunneling is allowed. The steps in the hysteresis loops, denoting quantum tunneling, are a characteristic feature of SMMs, whereas the signature of exchange bias effects is a deviation of this zero-field step to $H \neq 0$. The hysteresis loops are affected by the pressure, as is evident through the significant reduction of the coercive field as well as the lowering of the remnant magnetization at $H = 0$. The coercivity at ambient pressure of $H_c = 1.35$ T was reduced to $H_c = 1.22$ T at an applied pressure of 0.2 GPa and further to 1.08 T at 0.74 GPa. The coercive field at the highest measured pressure (1.14 GPa) was $H_c = 0.91$ T (for a total difference of 0.44 T from ambient conditions). Therefore, the coercivity is clearly pressure-dependent, and this result can be interpreted as an effective reduction of the overall axial anisotropy.
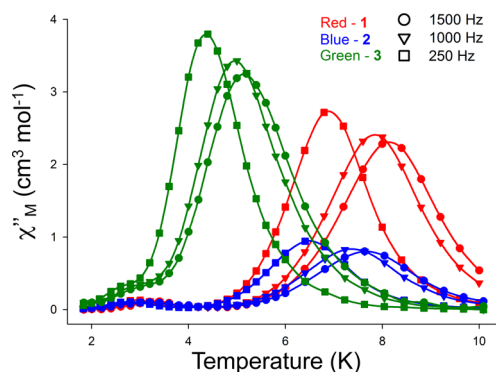
Figure 1. (A) Crystal structure of **1**, with *tert*-butyl groups omitted for clarity. (B) Core structure of **2**, with the peripheral carboxylates omitted for clarity. (C) Core structure of **3**, with the peripheral carboxylates omitted.

In contrast, Awaga and co-workers observed a decrease by as much as 50% of the quantum tunneling rate in $Mn_{12}Ac$, which resulted in an increase of the observed anisotropy barrier.[10] In addition, Gudel and co-workers used inelastic neutron scattering spectroscopy to study $Mn_{12}Ac$ and observed that the slow-relaxing species, which corresponds to the high-T peak in Figure 2, transforms with pressure to the fast-relaxing species (low-T peak) because of JT isomerization, where one of the JT axes is reoriented.[11] Our observations from the Mn_{12} chain species in the present work suggest that the model described by Gudel and Murrie seems to be more appropriate for our system,[11] and X-ray crystallography of **1** subjected to pressure is planned to test this conjecture.

The hysteresis data indicate saturation of the magnetization at all pressures. Steps are evident at zero- and nonzero-field values. Because of the superconducting effect of Pb, which dominates the low-field data ($H < \pm 100$ mT), we cannot conclusively discuss quantum bias effects or entanglement. Further magnetic and/or spectroscopic studies under pressure will shed light on the origin of the observed behavior and will be reported in due course.

Furthermore, in order to investigate the structure−property relationship in this family of Mn_{12} SMM chains, high-field/frequency electron paramagnetic resonance spectroscopy (HFEPR) was utilized. It is evident from the results in Table 1

Table 1. HFEPR Results for Complexes 1−3

	g_x/g_y	g_z	D (cm^{-1})	Mn^{III}−Mn^{III} (Å)
1	1.984	1.950	−0.495	10.0(1)
2	1.976	1.997	−0.482	9.7(1)
3	1.952	1.964	−0.461	8.1(1)

that there is some correlation between the Mn^{III}−Mn^{III} distance at the site of covalent linkage and the D value. It is not clear if this correlation has a physical meaning or if it is coincidental. It is worth noting that for complex **3**, in which the orientation of the clusters is different from that of the other chains, D has the lowest relative magnitude. Nevertheless, it is clear that the structure plays a major role in the material's properties.

In conclusion, we have covalently linked the Mn_{12} SMMs into 1D chains. This is the first family of linked chains of Mn_{12} SMMs produced utilizing a highly targeted method. This method is of particular value for further studies of linked Mn_{12} SMMs targeted at an extended family of multidimensional polymeric species. The physical properties of these systems could potentially be very exciting, especially if we are able to observe and/or control superposition/entanglement effects by modifying the linkers, and such studies have commenced. Furthermore, linking of SMMs into three-dimensional networks could result in SMM-based metal−organic frameworks,[12] a class of materials under growing interest for their potential to open new frontiers for SMM research.

■ ASSOCIATED CONTENT

Ⓢ Supporting Information

The Supporting Information is available free of charge on the ACS Publications website at DOI: 10.1021/acs.inorgchem.6b00058.

> Experimental and measurement details, additional figures, and HFEPR results (PDF)
> CIF files for **1−3** (CIF)

■ AUTHOR INFORMATION

Corresponding Author

*E-mail: c.lampropoulos@unf.edu.

Notes

The authors declare no competing financial interest.

■ REFERENCES

(1) Christou, G. *Polyhedron* **2005**, *24*, 2065−2075.
(2) Aromi, G.; Brechin, E. K. In *Single-molecule magnets and related phenomena*; Winpenny, R., Ed.; Springer: Heidelberg, Germany, 2006; pp 1−67.
(3) Bagai, R.; Christou, G. *Chem. Soc. Rev.* **2009**, *38*, 1011−1026.
(4) For a review, see: Friedman, J. R.; Sarachik, M. P. *Annu. Rev. Condens. Matter Phys.* **2010**, *1*, 109−128.
(5) (a) Wernsdorfer, W.; Aliaga-Alcalde, N.; Hendrickson, D. N.; Christou, G. *Nature* **2002**, *416*, 406−409. (b) Hill, S.; Edwards, R. S.; Aliaga-Alcade, N.; Christou, G. *Science* **2003**, *302*, 1015−1018. (c) Nguyen, T. N.; Shiddiq, M.; Ghosh, T.; Abboud, K. A.; Hill, S.; Christou, G. *J. Am. Chem. Soc.* **2015**, *137*, 7160−7168. (d) Nava, A.; Rigamonti, L.; Zangrando, E.; Sessoli, R.; Wernsdorfer, W.; Cornia, A. *Angew. Chem.* **2015**, *127*, 8901−8906.
(6) (a) Mowson, A. M.; Nguyen, T. N.; Abboud, K. A.; Christou, G. *Inorg. Chem.* **2013**, *52*, 12320−12322. (b) Lecren, L.; Wernsdorfer, W.; Li, Y.-G.; Vindigni, A.; Miyasaka, H.; Clerac, R. *J. Am. Chem. Soc.* **2007**, *129*, 5045−5051. (c) Katsenis, A. D.; Inglis, R.; Prescimone, A.; Brechin, E. K.; Papaefstathiou, G. S. *CrystEngComm* **2012**, *14*, 1216−1218. (d) Lin, P.-H.; Gorelsky, S.; Savard, D.; Burchell, T. J.; Wernsdorfer, W.; Clerac, R.; Murugesu, M. *Dalton Trans.* **2010**, *39*, 7650−7658.
(7) Lampropoulos, C.; Murugesu, M.; Harter, A. G.; Wernsdofer, W.; Hill, S.; Dalal, N. S.; Reyes, A.; Kuhns, P. L.; Abboud, K. A.; Christou, G. *Inorg. Chem.* **2013**, *52*, 258−272.
(8) Lis, T. *Acta Crystallogr., Sect. B: Struct. Crystallogr. Cryst. Chem.* **1980**, *36*, 2042−2046.
(9) Seiden, P. E. *Phys. Rev.* **1969**, *179*, 458−462.
(10) Murata, Y.; Takeda, K.; Sekine, T.; Ogata, M.; Awaga, K. *J. Phys. Soc. Jpn.* **1998**, *67*, 3014−3017.
(11) (a) Sieber, A.; Bircher, R.; Waldmann, O.; Carver, G.; Chaboussant, G.; Mutka, H.; Gudel, H.-U. *Angew. Chem., Int. Ed.* **2005**, *44*, 4239−4242. (b) Parois, P.; Moggach, S. A.; Sanchez-Benitez, J.; Kamenev, K. V.; Lennie, A. R.; Warren, J. E.; Brechin, E. K.; Parsons, S.; Murrie, M. *Chem. Commun.* **2010**, *46*, 1881−1883.
(12) Katsenis, A. D.; Brechin, E. K.; Papaefstathiou, G. S. In *Metal−Organic Framework Materials, Encyclopedia of Inorganic and Bioinorganic Chemistry*; Macgillivray, L. R., Lukehart, C., Eds.; John Wiley & Sons: New York, 2014; pp 245−258.